URSI GASS 2021, Rome, Italy, 28 August - 4 September 2021

Research on the Influence of Vehicle Body on the Characteristics of Vehicle Radiated Emission

Yingying Dong (1), Yinghong Wen(2), Dan Zhang(3) ,and Jinbao Zhang* (4)
Beijing Jiaotong University, Beijing, China, 100044

Abstract

The electromagnetic environment of the high-speed railway is very important to the high-speed railway operating system itself and the surrounding sensitive facilities. The electromagnetic environment directly affects the reliability of the electronic and electrical systems in this environment and the safety of high-speed rail transportation. Radiation emission is one of the important factors determining the electromagnetic environment of high-speed railways. Therefore, the overall vehicle radiation emission level of high-speed EMUs is not only an important indicator for evaluating the electromagnetic compatibility performance of high-speed EMUs, but also one of the key performance indicators that users must pay most attention to when they are exported. This paper will start with the analysis of the main influencing factors of the vehicle's radiated emissions, focusing on the influencing factors that cause the vehicle's radiated emissions to exceed the low frequency standard-the radiation emission current characteristics of the high-speed rail vehicle.

1 Introduction

The Chinese standard EMU is based on the CRH2 EMU design, and is a complete vehicle design formed through transformation and optimization. The traction power supply of the EMU adopts 25KV, 50Hz AC power supply. [1]In normal operation, the EMU uses a single bow to receive current, and the other pantograph is in a folded state. After the EMU obtains energy from the contact network through the pantograph and supplies it to the vehicle-mounted equipment, it flows into the steel rail through the grounding resistance and then through the grounding carbon brush, and flows into the ground through the through-line to send the traction back to the traction substation[2-4].

Through a large number of test results, it is found that the frequency of the power supply system is power frequency, and the frequency range of the vehicle's radiated emissions exceeds the standard is about several tens of kHz. This means that the radiated emissions of the entire vehicle are not directly caused by traction and power supply. It is directly caused by the transient disturbance of the equivalent circuit of the train. [3-5]The main sources of transient disturbances in the equivalent circuit of a train vehicle are: during the train operation, the pantograph network is offline and excessively equal, which will cause the transient equivalent of the train's equivalent circuit to be subject to transient steps or pulse disturbances and the internal nonlinearity of the traction system Response to transient disturbances.

Due to the high-voltage through cables, traction systems, and equipment cables on the roof, there are distribution parameters between the metal body and the body itself. When transient disturbances of different voltage sources occur in the equivalent circuit of the train, the voltage and current in the circuit cannot be quickly restored to a stable state, and a rich harmonic disturbance current is generated. [6-8]These disturbance currents propagate along the body of the vehicle, further causing the problem that the vehicle's radiation emission measurement results exceed the standard. Therefore, when studying the radiation emission characteristics of the entire vehicle, in addition to analyzing the radiation emission characteristics of the transient disturbance of the traction system, the radiation emission characteristics of the ground current of the vehicle body should also be studied.

2 Radiation emission prediction model of vehicle body distributed current

In the EMU, it is common for the low-voltage control line to run parallel to the high-voltage equipment line, and the wiring paths are close to the metal body. This makes the crosstalk coupling between the lines and the indirect crosstalk coupling through the metal car body very significant. Especially when the train is out of phase or a certain high-voltage equipment fails, the traction current will increase instantaneously, up to several thousand amps. At this time, due to the electromagnetic coupling between the core and the shielding layer, when the sudden change in the current in the core increases, it will cause overvoltage and overcurrent from the shielding layer to the car body.

The vehicle body induced current can be equivalent to a surface current induced on the vehicle body surface by a field generated by a power supply line near the surface of the vehicle body. As shown in Figure 1.

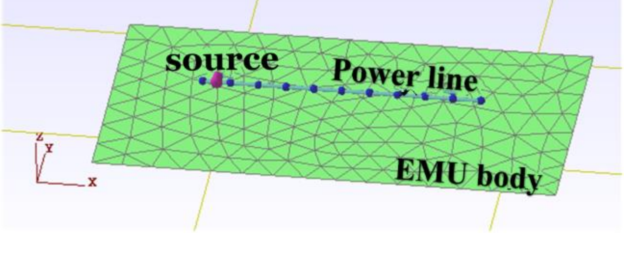

Figure 1. Equivalent model for calculating the induced current on the carriage

As a numerical calculation method for full-wave analysis of electromagnetic fields, the moment method can accurately analyze the current distribution on the conductor surface. Therefore, the equivalent surface current density J(r') and the equivalent surface charge density ρ(r') are used instead of the conductor surface. The scattering field generated by the conductor surface can be expressed as:

$$E^{sct}(r) = -j\omega A - \nabla\Phi \qquad (1)$$

Among them, the vector potential function A and the scalar potential are,

$$A(r) = \mu\int_{S'} G^A(r', r) J(r') ds' \qquad (2)$$

$$\Phi(r) = \frac{1}{\varepsilon}\int_{S'} G^{\Phi}(r', r)\,\rho(r') ds' \qquad (3)$$

According to the boundary conditions of the ideal conductor surface (Perfact Electric Conductor, PEC), the total electric field on the conductor surface can be expressed as the sum of the incident field $\boldsymbol{E}^{inc}$ and the scattered field $\boldsymbol{E}^{sct}$:

$$a_n \times [E^{inc}(r) + E^{sct}(r)] = 0 \qquad (4)$$

$\boldsymbol{G}^A(\boldsymbol{r'},\boldsymbol{r})$ is a scalar Green function, and $\boldsymbol{G}^{\phi}(\boldsymbol{r'},\boldsymbol{r})$ is a scalar Green function. In free space, both $\boldsymbol{G}^A(\boldsymbol{r'},\boldsymbol{r})$ and $\boldsymbol{G}^{\phi}(\boldsymbol{r'},\boldsymbol{r})$ can be defined as:

$$G_0(r, r') = \frac{e^{-jk|r-r'|}}{4\pi|r-r'|}, k = \omega\sqrt{\varepsilon_0\mu_0} \qquad (5)$$

The electric field integral equation (EFIE) can be obtained, that is, the relationship between the surface current density of the conductor and the incident field:

$$a_n \times \left[j\omega\mu\int_{s'} J(r') G^A(r', r) ds' + \frac{j}{\varepsilon\omega}\nabla\int_{s'} \nabla_{S'} \cdot J(r') G^{\Phi}(r', r) ds'\right] = a_n \times E^{inc}(r) \qquad (6)$$

In order to solve the surface current of the car body, a line segment grid is used to divide the line structure, and a triangular mesh is used to divide the surface structure. Therefore, the one-dimensional RWG basis function $\boldsymbol{f}_{1D}$ number is used to decompose the line current density, and the two-dimensional RWG basis function $\boldsymbol{f}_{2D}$ is used to decompose the vehicle body surface current density. as shown in picture 2 and picture 3.

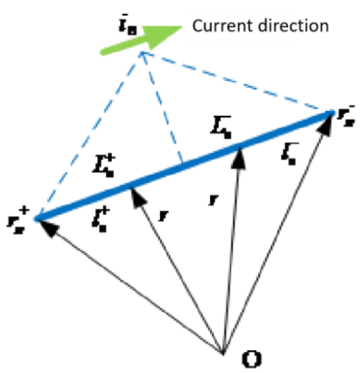

Figure 2. One-dimensional RWG basis functions

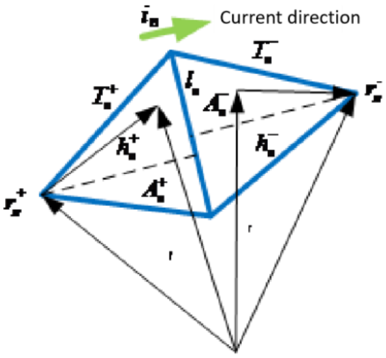

Figure 3. Two-dimensional RWG basis functions

Line current density can be expressed as:

$$J(r') = \frac{1}{2\pi a}\sum_{n=1}^{P} i_n f_n(r') \qquad (7)$$

P is the total number of common nodes of the line grid, a is the radius of the cable, and the current flowing through the nth common node.

Area current density can be expressed as,

$$J(r') = \sum_{n=1}^{M} j_n \quad f_n(r') = \sum_{n=1}^{M} \frac{i_n}{l_n} f_n(r') \qquad (8)$$

M is the total number of common edges of the triangular mesh, ln is the length of the nth common edge, and the current flowing in through the common edge.

According to FIG. 1, combined with formula 5, the common mode disturbance current source on the cable can be regarded as an equivalent voltage source on the cable by the incident field Einc voltage, as shown in FIG.4.

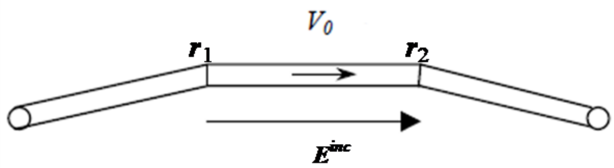

Figure 4. Equivalent voltage source

$$E^{inc} = \frac{V_0}{|r_1 - r_2|}(r_1 - r_2) \qquad (9)$$

$\boldsymbol{r}_1$, $\boldsymbol{r}_2$ are the fixed-point positions of the grid. According to the principle of equivalence, an ideal voltage source can be equivalent to the product of an ideal current source and the internal resistance r_{inp}:

$$V_0 = I_0 r_{inp} \qquad (10)$$

$r_{inp} = 10^{10}\,\Omega$.

Therefore, the line segment grid excitation source matrix $\mathbf{V^W}$ can be expressed as:

$$Vm = \langle f_m(r), E^{inc}(r)\rangle = \int_{L_m^+} \frac{1}{l_m^+}(r - r_m^+) \cdot \frac{V_0}{|r_1 - r_2|}(r_1 - r_2) dl - \int_{L_m^-} \frac{1}{l_m^-}(r - r_m^-) \cdot \frac{V_0}{|r_1 - r_2|}(r_1 - r_2) dl) \qquad (11)$$

The scattered field $\boldsymbol{E}^{sct}$ generated by the distributed current on the conductor surface can be expressed as:

$$E^{sct}(r) = -j\omega\mu \sum_{n=1}^{M} J_n \int_{S_n'} G^A(r,r') f_n(r') ds' - \frac{j}{\omega\varepsilon} \sum_{n=1}^{M} J_n \nabla \int_{S_n'} G^\phi(r,r') \nabla_{S'} \cdot f_n(r') ds' \quad (12)$$

$$\begin{aligned} I_{1n} &= \int_{S_n'} G^A(r,r') f_n(r') ds' \\ &= \int_{T_n^+} \frac{l_n}{2A_n^+}(r' - r_n^+) G_0(r,r') ds - \int_{T_n^-} \frac{-l_n}{2A_n^-}(r' - r_n^+) G_0(r,r') ds \\ &= \frac{l_n}{2}\left[\sum_{i=1}^{N^{2D}} \mathrm{w}_i^{2D} (r_i' - r_n^+) G_0(r,r') - \sum_{i=1}^{N^{2D}} \mathrm{w}_i^{2D} (r_i' - r_n^-) G_0(r,r')\right] \end{aligned} \quad (13)$$

$$\begin{aligned} I_{2n} &= \nabla \int_{S_n'} G^\varphi(r,r') \nabla_{s'} \cdot f_n(r') ds' \\ &= \int_{T_n^+} \frac{l_n}{A_n^+} \nabla G_0(r,r') ds + \int_{T_n^-} \frac{-l_n}{A_n^-} \nabla G_0(r,r') ds \\ &= l_n\left[\sum_{i=1}^{N^{2D}} \omega_i^{2D} \nabla G_0(r,r') - \sum_{i=1}^{N^{2D}} \omega_i^{2D} \nabla G_0(r,r')\right] \end{aligned} \quad (14)$$

The N^{2D} is the number of Gauss orthogonal integration points, and ω_i^{2D} is the Gauss orthogonal integration coefficient. l_n is the length of the nth common side.
Therefore, the scatter $\boldsymbol{E}^{sct}$ is

$$E^{sct}(r) = -\sum_{n=1}^{M} J_n \left(j\omega\mu I_{1n}(r) + \frac{j}{\omega\varepsilon} I_{2n}(r) \right) \quad (15)$$

3 Analysis of the influence of vehicle body distributed current on the radiation emission characteristics of the whole vehicle

Based on previous field tests on CRH2A, B, C, E, CRH380A, and CRH380AL EMU platforms, the main component of the ground current of high-speed EMUs comes from fluctuations in car body potential. Especially when the train is out of phase. This is because in the process of over-phase splitting, the train will experience the process of cutting off the load, opening the main circuit breaker, inert over-phase splitting, closing the main circuit breaker, and recovering power. Transient process of being cut off and causing over voltage. At this time, the transient current will enter the in-vehicle power supply system along the high-voltage cable on the roof. Due to the distributed capacitance between the high-voltage cable and the metal car body, the disturbance current on the cable will be coupled to the car body at the same time, resulting in the car body induced current. High-voltage coaxial cables are currently widely used in high-voltage electrical units on vehicles. This cable is laid from the pantograph along the roof to the compartment where each traction transformer is located, and each vehicle is connected using a high-voltage connector and a flexible cable, as shown in Figure 5.

$$E^{sct}(r) = -j\omega A - \nabla\Phi \quad (1)$$

Figure 5. Roof pantograph and cable of CRH2A

For the CRH2A type 8 marshalling EMU actually used, the high-voltage through cable runs through nearly 5 cars, each car is 24.5m long and the cable length exceeds 122.5m. The cross section of the high-voltage cable is shown in Figure 6.

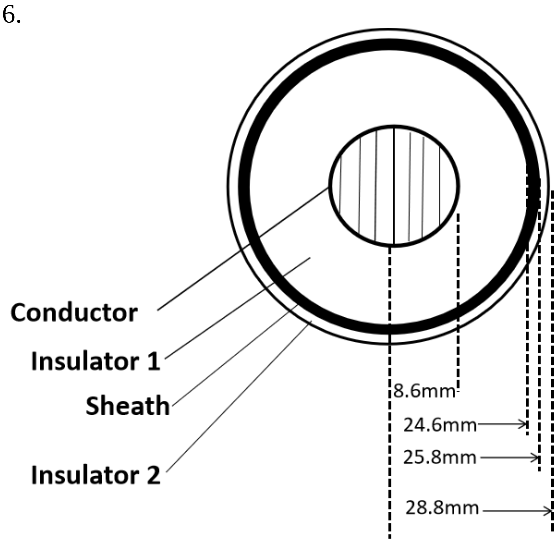

Figure 6. Cross section of high-voltage cable

The disturbance current on the high-voltage cable is shown in Figure 7.

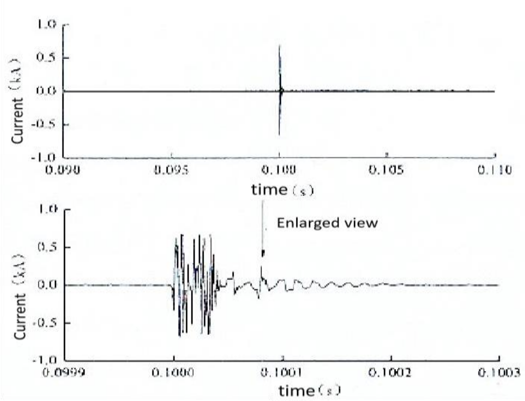

Figure 7. The disturbance current on the high-voltage cable

According to the calculation method of the radiation field generated by the vehicle body distributed current in Chapter 2, we can get the low-frequency magnetic field emission situation of the whole vehicle below 30MHz when the vehicle body distributed current is considered, as shown in Figure 8. It can be seen that when the train is over-phase, the magnetic field emission near 20MHz is close to the standard limit. The fundamental reason is that when the train is over-phase, the overcurrent on the high-voltage cable is coupled to the car body, and the overcurrent on the car body generates secondary radiation. Therefore, suppressing the electromagnetic disturbance on the high-voltage cables when the train is out of phase is the basis to solve the radiated emissions of the entire vehicle.

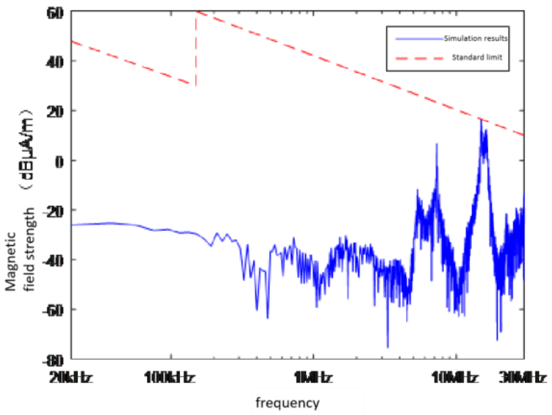

Figure 8. Magnetic field emission (10m, below30Mz)

4 Conclusion

Based on the test results of the vehicle's radiated emissions, the influential factors of the vehicle's radiated emissions were analyzed in depth. It is concluded that when there are transient disturbances of different voltage sources in the traction power supply system, the disturbance current is propagated along the vehicle body due to the existence of the distribution parameters of the high-voltage through cables, traction system, equipment cables and metal body on the roof, Causes the vehicle emission measurement results to exceed the standard. In order to analyze the influence of the vehicle body on the radiated emission of the entire vehicle, the moment method was used to decompose the integral equation of the electric field, and a vehicle body distributed current model and a vehicle body distributed current radiation emission model were established. Taking the radiated emission of the distributed current on the roof of the train as an example, the influence of the vehicle body on the radiated emission characteristics of the entire vehicle is analyzed in depth.

The root cause is that when the train is over-phase, the overcurrent on the high-voltage cable is coupled to the car body, and the overcurrent on the car body generates secondary radiation. Therefore, suppressing the electromagnetic disturbance on the high-voltage cables when the train is out of phase is the basis to solve the radiated emissions of the entire vehicle.

5 Acknowledgements

Thanks to Professor Yinghong Wen, Teacher Dan Zhang, and Teacher Jinbao Zhang for their rigorous academic teaching and scientific research assistance. This work is supported by the basic scientific research business expenses of Beijing Jiaotong University(No.2020JBZD010), and the Pre-research on National Major Projects of Sichuan-Tibet Railway (No.2019CZ001).

6 References

1. BS EN50121-2:2017. Railway applications —Electromagneticcompatibility —Part 2: Emissions of the whole railway system to the outside world.

2. Cesario P , Sciutto G , Rossi C , et al. Digital simulation for solution of oscillatory overvoltage problems in AC railroad electrification[C]/ IET, 2002.

3. Wang Yankun. Research on the interference analysis and protection of the electrified traction backflow on the signal control system [D] .Lanzhou Jiaotong University, 2012.

4. S. Ranganathan, D. G. Beetner, R. Wiese and T. H. Hubing, "An expert system architecture to detect system-level automotive EMC problems," 2002 IEEE, MN, USA, 2002, pp. 976-981 vol.2, doi: 10.1109/ISEMC.2002.1032828.

5. Yue Xu, Yinghong Wen, Xiaodong He and Dong Liu, "Analysis on the characteristics of radiation emission of EMU," 2015 IEEE 6th (MAPE), Shanghai, 2015, pp. 487-490, doi: 10.1109/MAPE.2015.7510364.

6. S. Frei, R. G. Jobava and D. Topchishvili, "Complex approaches for the calculation of EMC problems of large systems," 2004 International Symposium on Electromagnetic Compatibility (IEEE Cat. No.04CH37559), Silicon Valley, CA, USA, 2004, pp. 826-831 vol.3, doi: 10.1109/ISEMC.2004.1349929.

7. S. Ranganathan, D. G. Beetner, R. Wiese and T. H. Hubing, "An expert system architecture to detect system-level automotive EMC problems," 2002 IEEE International Symposium on Electromagnetic Compatibility, Minneapolis, MN, USA, 2002, pp. 976-981 vol.2, doi: 10.1109/ISEMC.2002.1032828.

8. Surajit Midya, Rajeev Thottappillil, An overview of electromagnetic compatibility challenges in European Rail Traffic Management System, Transportation Research Part C: Emerging Technologies, Volume 16, Issue 5, 2008, Pages 515-534, ISSN 0968-090X.